

## One-step synthesis of Ta<sub>3</sub>N<sub>5</sub> nanorod photoanode from Ta plate and NH<sub>4</sub>Cl powder for photoelectrochemical water oxidation

Yao Xiang,<sup>ab</sup> Boyang Zhang,<sup>ab</sup> Jintao Liu,<sup>ab</sup> Shanshan Chen,<sup>c</sup> Takashi Hisatomi,<sup>c</sup> Kazunari  
Domen,<sup>cd</sup> and Guijun Ma<sup>\*a</sup>

a. School of Physical Science and Technology, ShanghaiTech University, Shanghai 201210,  
China

b. University of Chinese Academy of Sciences, Beijing 100049, China

c. Research Initiative for Supra-Materials, Shinshu University, 4-17-1 Wakasato, Nagano-  
shi, Nagano 380-8553, Japan

d. Office of University Professors, The University of Tokyo, 7-3-1 Hongo, Bunkyo-ku,  
Tokyo 113-8656, Japan

## Contents

Details of the experiments and discussions.

**Figure S1.** EDS elemental mapping images of a cross-section of the Ta<sub>3</sub>N<sub>5</sub>/Ta sample.

The scale bars are 500 nm. **a)** BSE image, **b)** N K series, **c)** O K series, **d)** Ta K series.

**Figure S2.** FTIR spectra of the products in the quartz tube after reaction. The absorption peaks were assigned to gaseous HCl species.

**Figure S3.** Left: XRD patterns of **(a)** Ta plate and the samples prepared by reaction of Ta plate and NH<sub>4</sub>Cl powder in vacuo at **(b)** 1053 and **(c)** 703-1053 K. Ta<sub>3</sub>N<sub>5</sub> peaks are indexed. Asterisks represent the other TaN<sub>x</sub> signals. Right: the temperature programs for preparation of sample **(b)** and **(c)**.

**Figure S4.** Current-potential curves for (a) pristine Ta<sub>3</sub>N<sub>5</sub>, (b) Co(OH)<sub>x</sub>/Ta<sub>3</sub>N<sub>5</sub> and (c) Ni(OH)<sub>x</sub>/Co(OH)<sub>x</sub>/Ta<sub>3</sub>N<sub>5</sub> photoanodes under AM 1.5G simulated solar light in 0.5 M Na<sub>2</sub>B<sub>4</sub>O<sub>7</sub> aqueous solution (pH = 13). The Ta<sub>3</sub>N<sub>5</sub> photoanode was prepared with the temperature program of 703-1053 K.

**Table S1.** The amount of precursors and the constituents detected after the reaction of synthesizing Ta<sub>3</sub>N<sub>5</sub> from Ta and NH<sub>4</sub>Cl.

**Table S2.** Synthesis processes of Ta<sub>3</sub>N<sub>5</sub> photoanodes

## Supporting Information

### Experimental section

#### Preparation of Ta<sub>3</sub>N<sub>5</sub>/Ta

A metal tantalum sheet (The Nilaco company) with an area of 25 × 7.5 mm<sup>2</sup> and a thickness of 0.1 mm was taken as a Ta precursor. NH<sub>4</sub>Cl was used to provide nitrogen source for nitridation reaction. Before experiment, the NH<sub>4</sub>Cl powder was dehydrated by heating in a muffle furnace at 473 K for 2 h in air. The tantalum sheet was sequentially cleaned in acetone, ethanol, and ultrapure water under sonication and dried in nitrogen stream. In a typical procedure, the tantalum metal sheet and 15 mg of NH<sub>4</sub>Cl powder were put into a quartz tube ( $\phi$ 8 mm). Then, the tube was sealed by flame after evacuating to an approximate pressure of 1.3 Pa. The length of the filled tube was around 80 mm equaling to an inner volume of 4 cm<sup>3</sup>. The samples were heated via a two-step temperature program with maintaining at 673–733 K for 2 h in the first step and 1023–1063 K for 2 h in the second one, and finally cooled down to room temperature naturally. The heating rate is 2.5 K min<sup>-1</sup>. The obtained Ta<sub>3</sub>N<sub>5</sub>/Ta thin films were washed with ultra-pure water before usage.

#### Surface modification with Co(OH)<sub>x</sub> and Ni(OH)<sub>x</sub> on Ta<sub>3</sub>N<sub>5</sub> film

Before the PEC measurement, Co(OH)<sub>x</sub> and Ni(OH)<sub>x</sub> were deposited sequentially on the prepared Ta<sub>3</sub>N<sub>5</sub>/Ta film as oxygen evolution catalysts. For the Co(OH)<sub>x</sub> deposition, the

Ta<sub>3</sub>N<sub>5</sub>/Ta samples were immersed in an aqueous solution containing 0.2 M CoSO<sub>4</sub> and 6.28 mM NH<sub>3</sub>·H<sub>2</sub>O for 30 min, and then washed with copious deionized water. The Ni(OH)<sub>x</sub> layer was loaded over the above Co(OH)<sub>x</sub>/Ta<sub>3</sub>N<sub>5</sub>/Ta through a electrodeposition route, in which 0.025 M NiSO<sub>4</sub> solution was used as an electrolyte in an undivided cell. An applied potential of 1.16 V vs Ag/AgCl was held until the charge passed through the outer circuit reached about 25 mC cm<sup>-2</sup>.

### **Materials characterization**

The morphologies of the samples were examined using a field-emission scanning electron microscope (SEM, JEOL JSM-7800F Prime) with an energy dispersive spectrometer (EDS) detector. The crystal structures of samples were investigated by X-ray diffraction (XRD, Bruker D8 Advance) with Cu K $\alpha$  radiation.

### **PEC measurements of Ta<sub>3</sub>N<sub>5</sub>/Ta photoelectrodes**

The PEC tests were conducted in a three-electrode system with a potentiostat (Gamry, Interface 1000T) under simulated AM 1.5G solar light irradiation (100 mW·cm<sup>-2</sup>, SAN-EI ELECTRIC, Class AAA Solar simulator). The fabricated Ta<sub>3</sub>N<sub>5</sub>, a platinum wire, and a Ag/AgCl (saturated potassium chloride) were used as working, counter and reference electrodes, respectively. Unless otherwise noted, 0.5 M Na<sub>2</sub>B<sub>4</sub>O<sub>7</sub> aqueous solution with pH adjusted to 13 by adding NaOH was used as an electrolyte after saturation with Ar gas

for 10 min. The measured potentials were converted to V vs RHE ( $E_{\text{RHE}} = E_{\text{Ag/AgCl}} + 0.244 \text{ V} + 0.059 \text{ V} \times \text{pH}$ ). The photocurrent was measured by linear sweep voltammetry with a scan rate of  $10 \text{ mV s}^{-1}$ . The light was irradiated from the front side of electrodes for all cases. Incident photon-to-current efficiency (IPCE) was measured under monochromatic light irradiation, provided by a tungsten lamp equipped with a monochromator. The light intensity was obtained using a calibrated Si photodiode.

The amount of evolved oxygen was determined through operation in a three electrode system with a potentiostat (Interface 1000T, Gamry) at a potential of 1.0 V vs RHE in a closed configuration, in which the produced gases were analyzed by an online gas chromatograph (Agilent Technologies Inc., 490 Micro GC) using a thermal conductivity detector (TCD).

### **Analysis of the products**

After the calcination of the quartz tube containing Ta metal plate and  $\text{NH}_4\text{Cl}$  powder, the products were characterized using a Fourier-transform infrared (FTIR) instrument before the quartz tube was opened. The FTIR spectra were obtained in a transmission mode with a VERTEX 70 spectrometer by averaging 64 scans at a resolution of  $2 \text{ cm}^{-2}$ . After that, the quartz tube was placed inside a soft plastic tube with Ar gas continuously flowing from one end and purging into 100 ml water at the other end. After the quartz tube was broken inside the plastic tube, the pH of the water was decreased owing to dissolution of HCl. The amount of HCl was calculated based on the change of the pH value. In a similar operation, the amount of hydrogen and nitrogen in the quartz tube were detected by connecting the

plastic tube to a gas chromatograph (GC). In this case, the HCl was trapped by a 1M NaOH solution before the sampling using a GC. The experimental data are summarized in Table S1.

### **Summarization of the processes of synthesizing Ta<sub>3</sub>N<sub>5</sub>**

Table S2 summarizes several methods typically applied to synthesizing Ta<sub>3</sub>N<sub>5</sub> photoanodes. In the early research, Ta<sub>3</sub>N<sub>5</sub> electrodes were fabricated by physically stacking the particle precursor on a conductive substrate (such as FTO) using paste or electrophoretic deposition (EPD), etc.<sup>1</sup> The high resistance between particle/particle and particle/substrate seriously inhibited the charge transport on Ta<sub>3</sub>N<sub>5</sub>. Abe and coworkers found that a post-necking treatment resulted in improvement of the photocurrent of Ta<sub>3</sub>N<sub>5</sub> electrode due to the facilitation of electron transport between electrode particles (entry 1). After that, a more efficient particle transfer (PT) method (entry 2) was developed, by which a mono-particle layer of Ta<sub>3</sub>N<sub>5</sub> was directly embedded in a metal substrate to improve the conductivity.<sup>2</sup> Both entry 1 and 2 are *ex situ* method that is the preparation and deposition of Ta<sub>3</sub>N<sub>5</sub> particles are separated. An *in situ* growth of Ta<sub>3</sub>N<sub>5</sub> is generally supposed to further improve the conductivity. In this case, by employing a Ta-containing conductive substrate as the precursor of nitridation, the Ta<sub>3</sub>N<sub>5</sub> particles are chemically bonded to the substrate in a molecular-level (entry 3 to 9).<sup>3</sup> As shown in table 1, the photocurrent obtained from the *in situ* growth method is averagely higher than the *ex situ* one. At present, the top two currents produced over Ta<sub>3</sub>N<sub>5</sub> photoanode were reported from entry 4 and 7.<sup>4,7</sup> Except the conductivity, morphology is another key factor in determining the activity through affecting light absorbance, bulk charge transfer efficiency, and number of reactive surface

sites, etc. Of those works related to the morphology design, TaO<sub>x</sub> nanotube and nanorod precursors were prepared by a widely applied anodization (entry 5 and 6) or a recently-reported magnetron glancing angle deposition (entry 7) technique.<sup>5,6,7</sup> After high-temperature nitridation in NH<sub>3</sub> flow, the nanostructures of the 1D TaO<sub>x</sub> precursor were kept in the Ta<sub>3</sub>N<sub>5</sub> product. From entry 1 to 7, it can be found that the use of TaO<sub>x</sub> precursor necessitates the use of NH<sub>3</sub> and the multi-step operation during preparation of Ta<sub>3</sub>N<sub>5</sub>. Li's group reported a carbonate-assisted one-step synthesis of Ta<sub>3</sub>N<sub>5</sub> films (entry 8).<sup>8</sup> This method enabled the direct synthesis of high-oxidation-state metal nitride films from metal precursors under ammonia flow, and the prepared Ta<sub>3</sub>N<sub>5</sub> electrode exhibited promising water splitting performance. In case of using TaO<sub>x</sub> as precursor, the temperatures for synthesizing Ta<sub>3</sub>N<sub>5</sub> are generally higher than 1100 K so as to break down the Ta-O bond. Compared with the previous reports, our work (entry 9) is featured with one-step, *in situ*, low-temperature (*ca.* 200 K lower than before) and none-NH<sub>3</sub> synthesis of nanostructured Ta<sub>3</sub>N<sub>5</sub> photoanode.

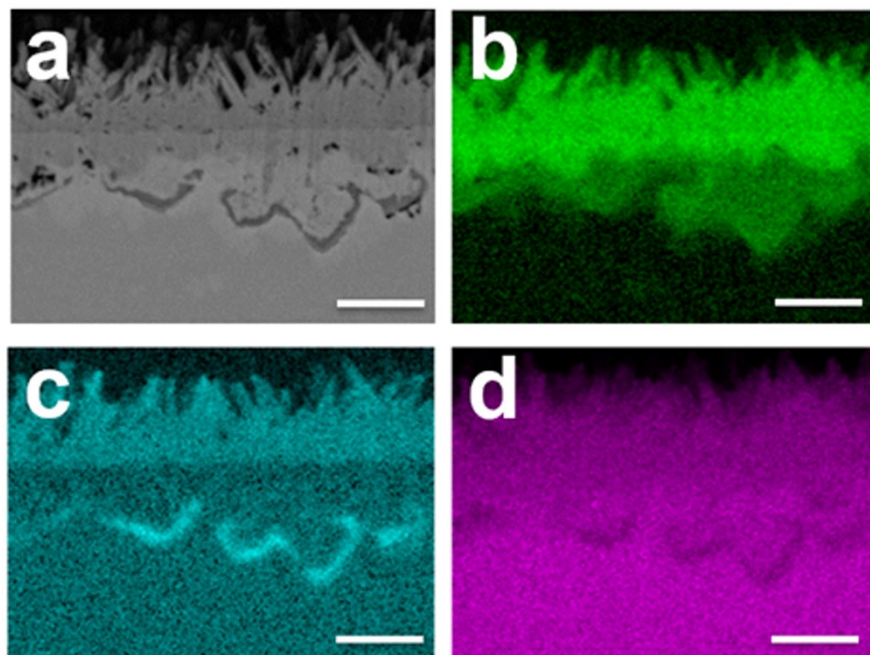


**Figure S1.** EDS elemental mapping images of a cross-section of the Ta<sub>3</sub>N<sub>5</sub>/Ta sample. The scale bars are 500 nm. **a)** BSE image, **b)** N K series, **c)** O K series, **d)** Ta K series.



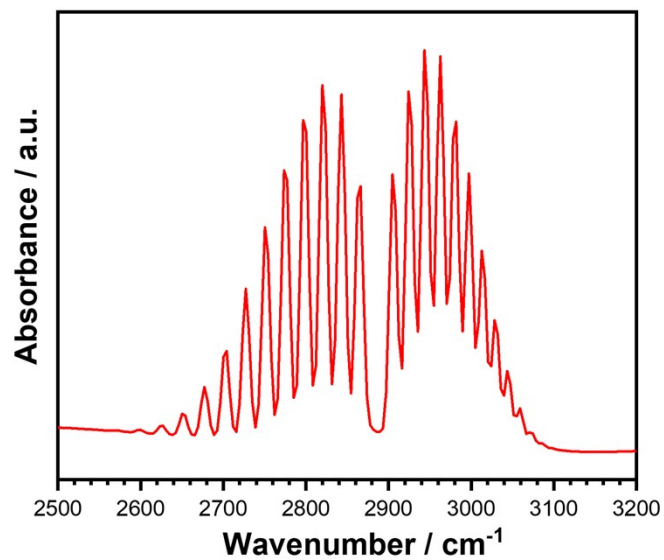


**Figure S2.** FTIR spectra of the products in the quartz tube after reaction. The absorption peaks were assigned to gaseous HCl species.

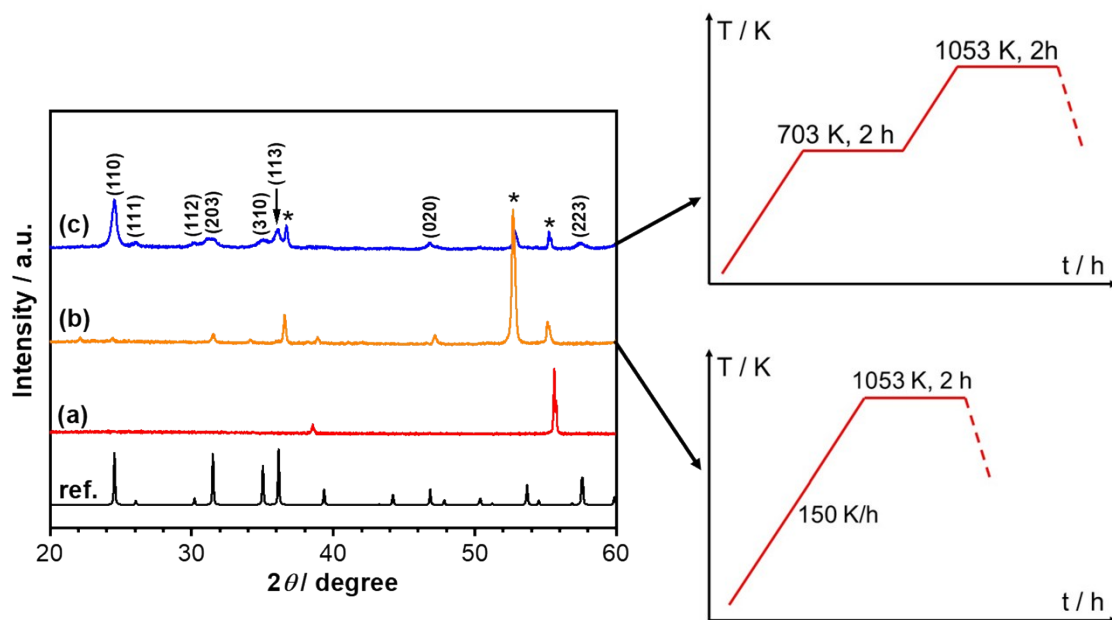


**Figure S3.** Left: XRD patterns of **(a)** Ta plate and the samples prepared by reaction of Ta plate and  $\text{NH}_4\text{Cl}$  powder in vacuo at **(b)** 1053 and **(c)** 703-1053 K.  $\text{Ta}_3\text{N}_5$  peaks are indexed. Asterisks represent the  $\text{TaN}_x$  signals. Right: the temperature programs for preparation of sample **(b)** and **(c)**.

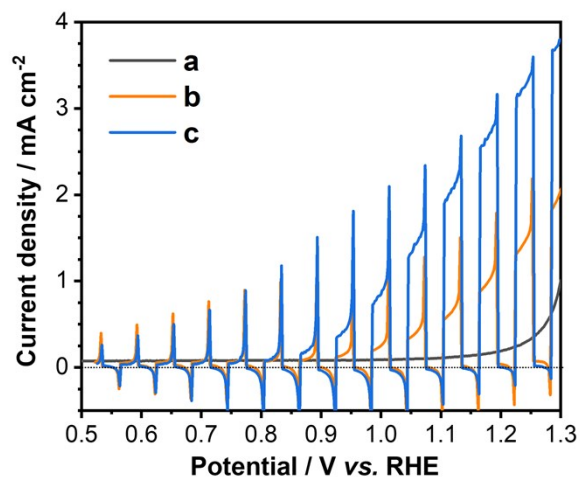


**Figure S4.** Current-potential curves for (a) pristine Ta<sub>3</sub>N<sub>5</sub>, (b) Co(OH)<sub>x</sub>/Ta<sub>3</sub>N<sub>5</sub> and (c) Ni(OH)<sub>x</sub>/Co(OH)<sub>x</sub>/Ta<sub>3</sub>N<sub>5</sub> photoanodes under AM 1.5G simulated solar light in 0.5 M Na<sub>2</sub>B<sub>4</sub>O<sub>7</sub> aqueous solution (pH = 13). The Ta<sub>3</sub>N<sub>5</sub> photoanode was prepared with the temperature program of 703-1053 K.

**Table S1.** The amount of precursors and the constituents detected after the reaction of synthesizing Ta<sub>3</sub>N<sub>5</sub> from Ta and NH<sub>4</sub>Cl.

Precursors	Amount of substance ( $\mu\text{mol}$ )	The reaction products	Amount of substance ( $\mu\text{mol}$ )
Ta metal plate	1700 $\pm$ 100	HCl	140 $\pm$ 20
NH <sub>4</sub> Cl powder	280 $\pm$ 15	H <sub>2</sub>	220 $\pm$ 20
		N <sub>2</sub>	65 $\pm$ 10
		Ta <sub>3</sub> N <sub>5</sub>	1 $\pm$ 0.1
		Residual NH <sub>4</sub> Cl <sup>a</sup>	140 $\pm$ 20

(<sup>a</sup>the amount was obtained by subtracting the amount of HCl from the NH<sub>4</sub>Cl precursor)

**Table S2** Synthesis processes of Ta<sub>3</sub>N<sub>5</sub> photoanodes

Entry	Synthesis processes	Total steps	NH <sub>3</sub> flow (mL min <sup>-1</sup> )	Temp. (K)	In/ex situ	J <sub>photo</sub> (mA cm <sup>-2</sup> ) <sup>e</sup> at 1.23 V <sub>RHE</sub>	Ref.
1 <sup>a</sup>	Ta <sub>2</sub> O <sub>5</sub> $\xrightarrow{\text{NH}_3}$ Ta <sub>3</sub> N <sub>5</sub> $\xrightarrow{\text{EPD, necking}}$ Ta <sub>3</sub> N <sub>5</sub> /FTO	2	500	1123	ex situ	3	1
2 <sup>b</sup>	Ta <sub>2</sub> O <sub>5</sub> $\xrightarrow{\text{NH}_3}$ Ta <sub>3</sub> N <sub>5</sub> $\xrightarrow{\text{PT}}$ Ta <sub>3</sub> N <sub>5</sub> /Ta/Ti	2	100	1173	ex situ	3.5	2
3	Ta $\xrightarrow{\text{Sputter}}$ TaO <sub>x</sub> /Ta $\xrightarrow{\text{NH}_3}$ Ta <sub>3</sub> N <sub>5</sub> /Ta	2	100	1113	in situ	2	3
4	Ta $\xrightarrow{\text{Hydrothermal}}$ NaTaO <sub>3</sub> /Ta $\xrightarrow{\text{NH}_3}$ Ta <sub>3</sub> N <sub>5</sub> /Ta	2	250	1223	in situ	12.1	4
5 <sup>c</sup>	Ta $\xrightarrow{\text{Anodization}}$ Ta <sub>2</sub> O <sub>5</sub> nr/Ta $\xrightarrow{\text{NH}_3}$ Ta <sub>3</sub> N <sub>5</sub> nr/Ta	2	100	973	in situ	—	5
6 <sup>d</sup>	Ta $\xrightarrow{\text{Anodization}}$ Ta <sub>2</sub> O <sub>5</sub> nr/Ta $\xrightarrow{\text{NH}_3}$ Ta <sub>3</sub> N <sub>5</sub> nr/Ta	4	10	1273	in situ	5	6
7 <sup>d</sup>	Ta $\xrightarrow{\text{Sputter}}$ TaO <sub>x</sub> nr/Ta $\xrightarrow{\text{NH}_3}$ Ta <sub>3</sub> N <sub>5</sub> nr/Ta	2	250	1253	in situ	9.95	7
8	Ta $\xrightarrow{\text{CO}_2 + \text{NH}_3}$ Ta <sub>3</sub> N <sub>5</sub> /Ta	1	250	1173	in situ	8	8
9 <sup>d</sup>	Ta+NH <sub>4</sub> Cl $\xrightarrow{\text{Vacuum heating}}$ Ta <sub>3</sub> N <sub>5</sub> nr/Ta	1	No	953	in situ	3.2	This work

(<sup>a</sup>EPD: Electrophoretic deposition, <sup>b</sup>PT: Particle transfer, <sup>c</sup>nr: Nanotube, <sup>d</sup>nr: Nanorod, <sup>e</sup>Under AM 1.5 solar simulator)

## References

- 1 M. Higashi, K. Domen and R. Abe, *Energy Environ. Sci.*, 2011, **4**, 4138–4147.
- 2 C. Wang, T. Hisatomi, T. Minegishi, M. Nakabayashi, N. Shibata, M. Katayama and K. Domen, *Chem. Sci.*, 2016, **7**, 5821–5826.
- 3 D. Yokoyama, H. Hashiguchi, K. Maeda, T. Minegishi, T. Takata, R. Abe, J. Kubota and K. Domen, *Thin Solid Films*, 2011, **519**, 2087–2092.
- 4 G. Liu, S. Ye, P. Yan, F. Xiong, P. Fu, Z. Wang, Z. Chen, J. Shi and C. Li, *Energy Environ. Sci.*, 2016, **9**, 1327–1334.
- 5 X. Feng, T. Latempa, J. Basham, G. Mor, O. Varghese and C. Grimes, *Nano Lett.*, 2010, **10**, 948–952.
- 6 Y. Li, T. Takata, D. Cha, K. Takanabe, T. Minegishi, J. Kubota and K. Domen, *Adv. Mater.*, 2013, **25**, 125–131.
- 7 Y. Pihosh, T. Minegishi, V. Nandal, T. Higashi, M. Katayama, T. Yamada, Y. Sasaki, K. Seki, Y. Suzuki, M. Nakabayashi, M. Sugiyama and K. Domen, *Energy Environ. Sci.*, 2020, **13**, 1519–1530.
- 8 T. Fang, H. Huang, J. Feng, Y. Hu, Y. Guo, S. Zhang, Z. Li and Z. Zou, *Sci. Bull.*, 2018, **63**, 1404–1410.